Key Points:
- Current and charge density measurements of two upward leaders induced by the same downward leader
- Upward leaders alternate their progression during initial propagation
- Current pulses of upward leaders increase intensity and synchronize right before attachment

Correspondence to:
M. M. F. Saba,
marcelo.saba@inpe.br

Author Contributions:
Conceptualization: Marcelo M. F. Saba
Data curation: Paola B. Lauria, Carina Schumann, Felipe de L. Mantovani
Formal analysis: Marcelo M. F. Saba, Paola B. Lauria, José Claudio de O. Silva, Felipe de L. Mantovani
Investigation: Marcelo M. F. Saba, Paola B. Lauria, Carina Schumann, José Claudio de O. Silva
Methodology: Marcelo M. F. Saba, Paola B. Lauria, Carina Schumann, José Claudio de O. Silva
Project Administration: Marcelo M. F. Saba
Supervision: Marcelo M. F. Saba
Validation: Marcelo M. F. Saba, Paola B. Lauria, José Claudio de O. Silva
Visualization: Paola B. Lauria, Carina Schumann, Felipe de L. Mantovani
Writing – original draft: Marcelo M. F. Saba

Upward Leaders Initiated From Instrumented Lightning Rods During the Approach of a Downward Leader in a Cloud-To-Ground Flash

Marcelo M. F. Saba[1] , **Paola B. Lauria[1], Carina Schumann[2], José Claudio de O. Silva[3], and Felipe de L. Mantovani[1]**

[1]INPE—National Institute for Space Research, São José dos Campos, Brazil, [2]JLRL University of the Witwatersrand, Johannesburg, South Africa, [3]APTEMC, São José dos Campos, Brazil

Abstract In this paper we analyze electric-field and current measurements of upward leaders induced by a downward negative lightning flash that struck a residential building. The attachment process was recorded by two high-speed cameras running at 37,800 and 70,000 images per second and the current measured in two lightning rods. Differently from previous works, here we show, for the first time, current measurements of multiple upward leaders that after initiation propagate to connect the negative downward moving leader. At the beginning of the propagation of the leaders that initiate on the instrumented lightning rods, current pulses appear superimposed to a steadily increasing DC current. The upward leader current pulses increase with the approach of the downward leader and are not synchronized but present an alternating pattern. All 2D leader speeds are approximately constant. The upward leaders are slower than the downward leader speed. The average time interval between current pulses in upward leaders is close to the interstep time interval found by optical or electric field sensors for negative cloud-to-ground stepped leaders. The upward leaders respond to different downward propagating branches and, as the branches alternate in propagation and intensity, so do the leaders accordingly. Right before the attachment process the alternating pattern of the leaders ceases, all downward leader branches intensify, and consequently upward leaders synchronize and pulse together. The average linear densities for upward leaders (49 and 82 μC/m) were obtained for the first time for natural lightning.

Plain Language Summary The effectiveness of a lightning protection system depends on its efficiency to intercept the down coming leader of a cloud-to-ground lightning flash. The interception is usually done by an upward connecting leader that initiates from grounded structures, humans, or living beings that protrude from nearby ground. The understanding of the upward connecting leader and of the attachment process with the downward leader plays an important role in the determination of the zone of protection and therefore in the improvement of a lightning protection system. Unconnected upward leaders, that is, upward leaders that fail to connect the downward leader, are also of great importance in lightning protection. They can be large enough to cause damage to equipment vulnerable to sparks or induced currents, and enough to injure people from who it initiates. In this paper we analyze electric-field, speed, and current measurements of upward leaders induced by a downward negative lightning flash that struck a residential building. The attachment process was simultaneously recorded by two high-speed cameras, an electric-field sensor, and current sensors installed on two lightning rods. Differently from previous works we show, for the first time, current measurements of multiple upward leaders induced by the negative downward moving leader.

1. Introduction

Previously, we have reported high-speed video images of attachment process of three negative downward cloud-to-ground flashes to an ordinary residential building (Saba et al., 2017). As mentioned in the cited paper, the effectiveness of a lightning protection system (LPS) depends on its efficiency to intercept the down coming lightning leader which is related to its efficiency to emit upward connecting leaders (UCL). The understanding of the characteristics of an UCL and of the attachment process with the downward leader plays an important role in the determination of the volume or zone of protection of a LPS and in the improvement of LPS designs. Unconnected upward leaders (UUL), that is, those events that initiate an upward leader but fail to make contact with the downward leader, are also of great importance in lightning protection. They can be large enough to cause damage

Writing – review & editing: Marcelo M. F. Saba, Paola B. Lauria, Carina Schumann, José Claudio de O. Silva, Felipe de L. Mantovani

to equipment vulnerable to sparks or induced currents, and enough to injure people (Becerra & Cooray, 2009; Cooper & Holle, 2019).

Although a few current measurements of upward leaders have been reported from tall towers higher than 60 m (e.g., Arcanjo et al., 2019; Nag et al., 2021; Saba et al., 2015; Visacro et al., 2017a, 2017b for towers over mountains), from buildings (Saba et al., 2017), and from small structures (Schoene et al., 2008, vertical conductor of 7 m height), no current measurements of upward connecting leaders from common residential buildings have been reported in the literature. Besides, some of these past studies do not have electric-field and current measurements together with high-speed video observations which is crucial to visualize what is happening with the upward and downward leaders involved in the attachment process.

This study presents observational data of several positive upward leaders responding to the approach of the negative leader of a downward cloud-to-ground flash that strikes an instrumented lightning rod of a residential building. It is the first to report current measurements of two upward leaders induced by the same downward leader. The use of high-speed video images and electric field measurements reveal the nature of the physical process that is generating the currents measured on the vertical lightning rods on the top of buildings.

2. Instrumentation

The lightning attachment to the building was observed by two high-speed video cameras Vision Research Phantom v12 and v711 operating at 70,000 and 37,800 frames per second with exposure times of 13.55 and 25.85 μs and time intervals of 14.29 and 26.46 μs respectively (videos available in Supplementary Information, Saba, 2022). Image spatial resolution used for the flashes herein was 128×360 pixels and 368×416 pixels, respectively. They were positioned at 220 m from a pair of identical 14-story apartment buildings, named P1 and P2, located in São Paulo City (23.483°S, 46.728°W), Brazil (Figure 1a). Their steel reinforced concrete structures are used as natural LPS. Each building has a vertical lightning rod, and their tips are at a height of 52 m respective to ground level. All reported distances and speeds given by the analysis of the images from the high-speed videos were measured in 2D and therefore underestimated.

The electric field changes caused by the attachment process was measured by a flat plate antenna with an integrator and amplifier. The antenna was located on top of building P2 only 4 m away from the lightning rod that was struck by a cloud-to-ground lightning flash (see Figure 1a). A fiber-optic link was used to transmit the signal from the integrator/amplifier to the digitizer. The bandwidth of the system ranged from 306 Hz to 1.5 MHz. The physics sign convention is used when referring to the electric field and its change. The approach of a nearby negative leader produces positive electric field change, and a negative CG return stroke produces a negative field change.

One current transformer sensor (Pearson model 301-X) was installed on the lightning rod of each building. This current sensor is capable of recoding current up to 50,000 A with a useable rise time of 200 nanoseconds, a low frequency 3 dB cut-off of approximately 5 Hz and a high frequency 3 dB cut-off of approximately 2 MHz. The output of the sensor is split in two channels (20 and 50 dB attenuation over 50 Ω) and sent to a data acquisition system through a pair of fiber optic links. The sensitivity and the noise level of the current measurements used in the present work (20 dB channel) were 1.0 and ±5 A, respectively. Before installation, both sensors were tested and calibrated in a high voltage facility. The electric field and current were continuously recorded at a sampling rate of 5 MS/s. GPS antennas were used to synchronize all measurements and video images.

Data from lightning location systems (LLS) were used to obtain the polarity, the time, and an estimate of the peak current of the return stroke. A complete study on the accuracy of peak current estimation given by the LLS has not been performed yet. However, for one recent event of a cloud-to-ground flash that struck one of the buildings, the error was within 20% for the strokes that were correctly classified as cloud-to-ground. In that event, four strokes were detected by the LLS and they were directly measured by the current sensor installed in the vertical lightning rod to where the attachment occurred. Further information about these systems and their performance are given in Naccarato et al. (2012, 2017).

More information about the cameras, the locations of the two buildings and the topography of the terrain can be found in the previous work (Saba et al., 2017).
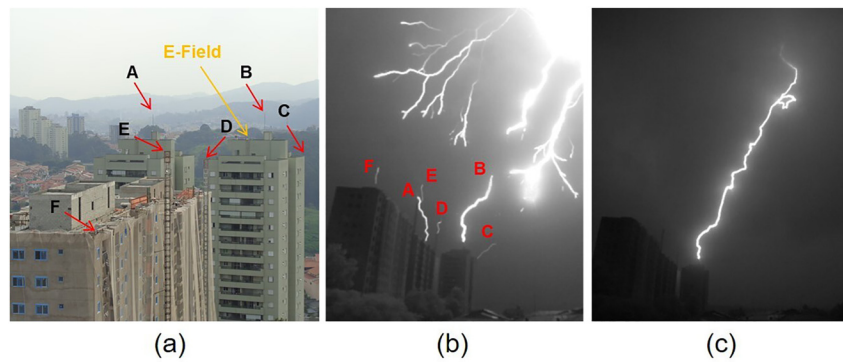
Figure 1. (a) structures A–F, where the upward leaders (also named A to F) are initiated. A and B indicate the tips of the instrumented lightning rods of buildings P1 and P2 respectively; (b) downward negative leader and positive upward leaders launched from the tip of the lightning rods and other nearby structures; (c) geometry of the return stroke channel.

3. Data

On 1 February 2017 a single-stroke negative cloud-to-ground lightning discharge struck the tip of the lightning rod B on building P2. According to the LLS, its peak return stroke current was −73 kA and occurred at 19:01:10.689307 (UT). During the approach of the stepped leader, a positive UCL was launched from the tip of the lightning rod B on building P2 together with five positive UULs from the vertical air-termination rod A of the other building (P1) and other nearby structures and corners (named C, D, E, F), as shown in Figure 1. The first upward leader to start a continuous propagation was the UCL leader. It started propagation when the downward leader closest tip was 132 m away from the tip of the P2 lightning rod where it started. The leaders had their origin at different distances from the electric field sensor and at different times ($t = 0$ s correspond to the attachment and beginning of return stroke in all tables and graphs). The leader types, 2D lengths (measured one frame before the occurrence of the return stroke), their horizontal distances from the electric field sensor, and inception times are shown in Table 1.

A sequence of images that shows the initiation and propagation of each upward leader is presented in Figure 2. The last image (number 24, $t = 0$ μs) shows the connection of the upward leader B with the downward leader.

Figure 3 presents the electric field measured during approximately 9 milliseconds before the occurrence of the return stroke. As mentioned before, in this work the electric field change is positive when negative charge over the sensor moves downward. Therefore, the electric field is intensified with the approach of the negative downward leader. However, as the positive leaders initiate and move upward, positive charges are positioned between the electric field sensor and the negative charge of the downward leader. Thus, the field is reversed with the initiation of the upward positive leaders and the occurrence of the return stroke.

Leaders A (UUL) and B (UCL) had their current measured by the current sensors installed on structures A and B in Figure 1a (lightning rod masts of buildings P1 and P2 respectively). Figure 4 shows the current measurements of upward connecting leaders and the electric field during 550 μs before the return stroke. In the plot, the numbers

Table 1
Structures That Initiated Upward Leaders, Leader Type, Length, Distance From the Electric Field Sensor and Time of Leader Inception

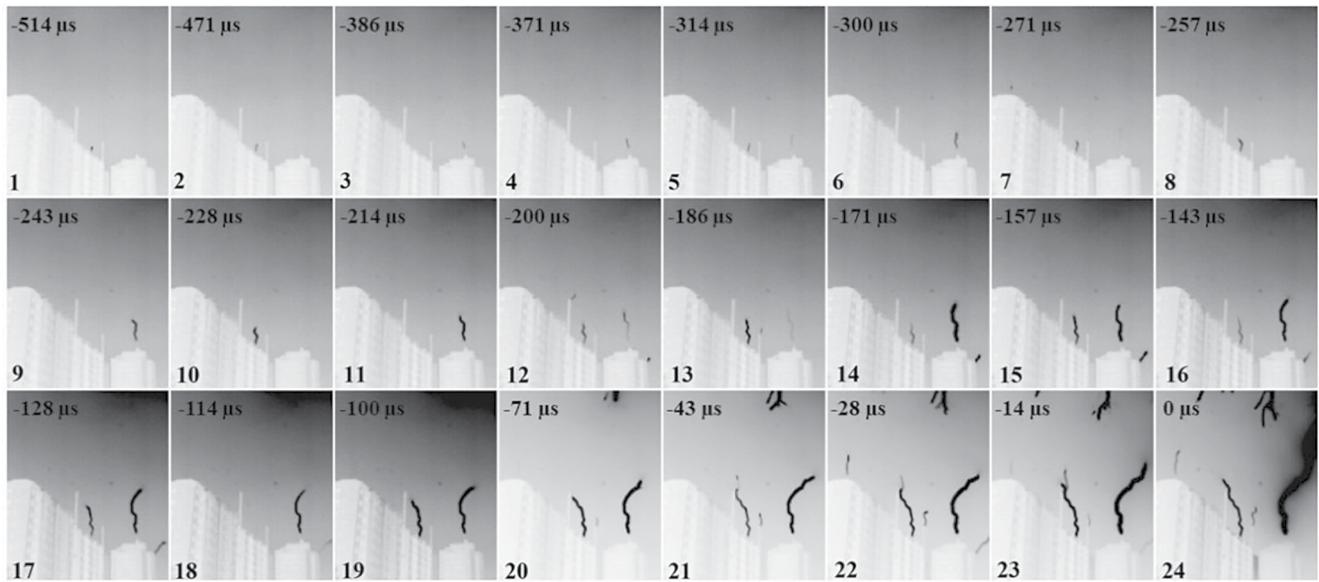| Structure	Structure type	Leader (type)	Leader maximum length (m)	Distance (m)	Time of leader inception (μs)
A	P1 lightning rod	A (UUL)	40.2	22.5	−314
B	P2 lightning rod	B (UCL)	50.4	4.0	−342
C	Building P2 corner	C (UUL)	15.0	14	−212
D	Construction elevator	D (UUL)	7.7	63	−106
E	Construction elevator	E (UUL)	7.2	105	−79
F	Construction corner	F (UUL)	4.7	141	−71

Figure 2. High-speed video image sequence of the upward leaders obtained at 70,000 frames per second. Each image contains the relative time to the image number 24 which shows the connection between the downward leader and upward leader B.

1 to 24 indicate the correspondent video images (shown in Figure 2) associated with the current pulses. Eighteen unipolar current pulses of some tens of amps (10's A) from both vertical masts are observed during this interval. The positive polarity of the pulses indicates an upward-directed transfer of positive charge. The highest current pulse (413 A; $t = -180$ μs) appears in leader B. Close to the occurrence of the return stroke, the pulses are superimposed on a DC current that was not considered when measuring the pulse current peak. The blue curve in Figure 4 traces the electric field changes during this time interval. The field starts saturated before pulse number 3 and saturates again with the occurrence of the return stroke.

4. Analysis and Discussion

4.1. Leader Speed

Based on the video images of both high-speed cameras it was possible to measure the 2D speed of leaders A and B, but also of other four UULs that are described in Table 1. The fastest upward leaders were the UCL
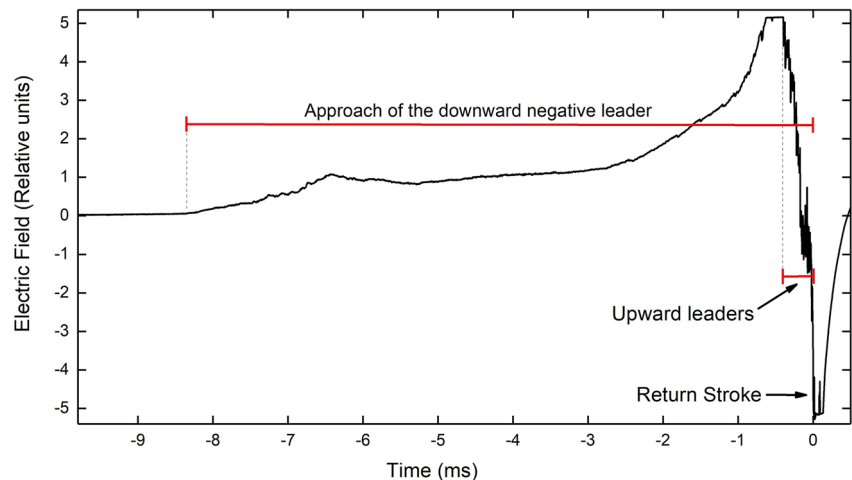

Figure 3. Electric field change caused by the approach of the negative downward leader, the initiation of the positive upward leaders, and the return stroke ($t = 0$ ms). The electric-field antenna was located 4 m away from the lightning rod struck by the flash (see Figure 1).
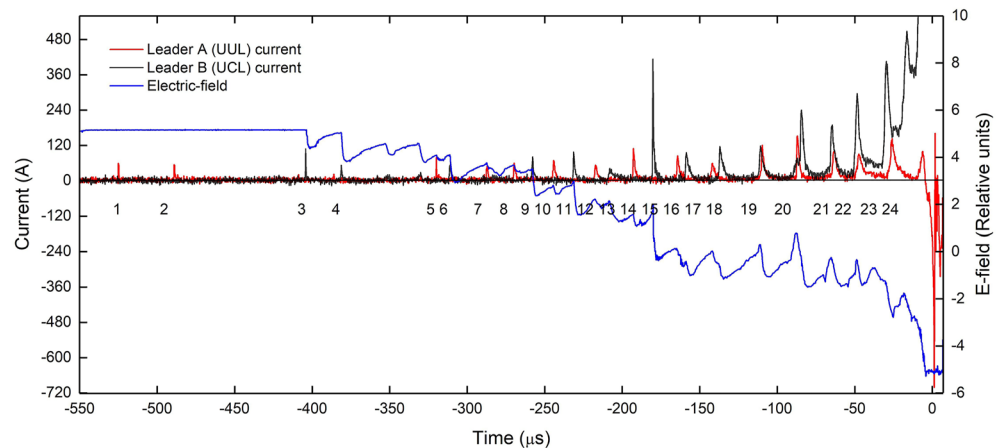
Figure 4. Measured current profile of an UCL from B and an UUL from A, and the electric field acquired during the event. The numbers 1 to 24 indicate the correspondent video images (shown in Figure 2) associated with the current pulses. The electric field was saturated before time −400 µs.

(leader B) and leader A, the closest UUL to the attachment point. All upward leaders propagated in an approximately constant speed (Figure 5). The downward leader that connected to leader B had also a constant speed but 2.0 times higher ($V_d = 28.5 \times 10^4$ m/s) than the speed of leader B (similar to the speed reported by Visacro et al. (2017a, 2017b) for four natural downward leaders before attachment and similar to the speed of the branches analyzed separately in Saba et al., 2022). This confirms what was found for other cases of attachment process in the same buildings by Saba et al. (2017) and similar buildings in Saba et al. (2022), that is, that contrary to what is observed in taller structures (Lu et al., 2013, 2015) and assumed in some leader propagation models (Rizk, 1990, 1994), speeds are approximately constant, and the speed of the downward leader is higher than the speed of the upward leaders (speed ratio between 2.0 and 5.5). Table S1 in Supporting Information S1 compares the speeds, speed ratios and other important characteristics for the case analyzed in this work with three other
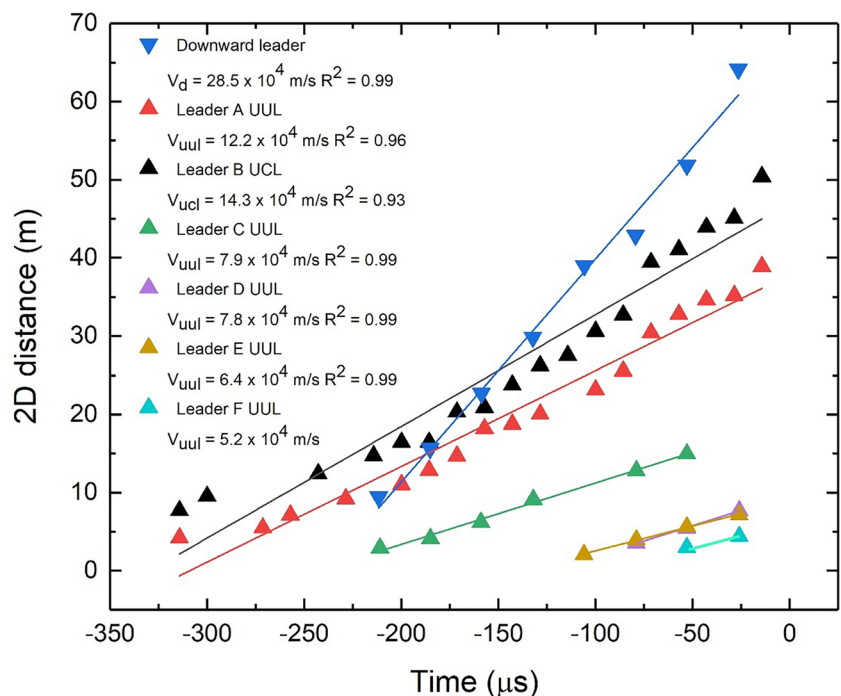

Figure 5. Leader propagation 2D speeds. No 2D distances were used for the interval $-26 < t < 0$ µs in the linear fit, to avoid uncertainties given by the last frame containing the return stroke.

Table 2
Height of Structure, Leader Length, Total Transferred Charge, and Linear Charge Density of Leaders A and B

Register	Structure	Structure height (m)	Leader length (m)	Total charge (mC)	Average linear charge density (μC/m)	Back flow current (A)
A (UUL)	Building	52	40.2	3.8	49	701
B (UCL)	Building	52	50.4	19.8[a]	82	–
Nag et al. (2021)	Tower	91.5	–	6.4[b]	–	283[b]
Visacro et al. (2010)	Tower	60[c]	–	–	–	~400 and ~800 A
Schoene et al. (2008)	Grounded conductor	7	–	–	–	~20 A
Chen et al. (2013)	Triggered lightning	266/159	387/549	–	155/62	–
Les Renardières (1977)	Laboratory discharges	–	–	–	20–50	–
Becerra and Cooray (2009)	Model	1.9	5.5	1.64	298	1,530

[a]Does not include the charge transfer due to the return stroke. [b]Median value of 8 measurements. [c]On top of a 280-m height mountain.

attachment processes in the same building as reported by Saba et al. (2017). These results were also compared to similar ones obtained by Tran and Rakov (2017; Table 2).

There is a significant increase in the speed of leader B (UCL) immediately before connection that suggests the final jump condition of the attachment process (also observed by Saba et al. (2017)). Leader B (UCL) propagated at a constant speed of 14.3×10^4 m/s and, during the last frame before connection, the speed increased to 51.4×10^4 m/s, 3.3 times higher than the previous average speed. Combining the time and length information given in the images from both cameras, the final jump speed (a combination of the downward and upward leader propagation, see e.g., discussion done by Saba et al. (2017)) was estimated to be higher than 640×10^4 m/s, that is, at least 45 times faster than the average speed of the upward leader. A similar speed was estimated by Tran and Rakov (2017) for the speed of the leader during the final jump (referred also as breakthrough phase in their work).

4.2. DC Background Current

Some distinct patterns were observed in the current plots of leaders A and B. Some preliminary luminosity and current pulses at the tip of the lightning rods were observed (the first four current pulses appearing in images 1–4 in Figure 2) a few tens of microseconds before the upward leaders start. Once the leaders start a continuous propagation (images 5–23 in Figure 2 after $t = -350$ μs), several current pulses occur superimposed on a continuously increasing DC current. The DC current of leader B (UCL) is much higher than the DC current of leader A (UUL) and both increase exponentially (Figure 6). A similar growth in current was modeled by Becerra and Cooray (2009), however no current pulses were present in their simulation and there was no statement about the exponential character of the current growth. A similar pattern was also observed by Visacro et al. (2017b).

4.3. Leader Pulses Alternation and Synchronism

One interesting feature that can be observed in Figures 2 and 4 is that although leaders A and B have their luminosity and current pulses increasing in time as the downward stepped leader approaches, they are not synchronized at the beginning (up to image 18 in Figure 2 and up to $t = -114$ μs in Figure 4).

It is also possible to observe from the high-speed video (Movies S1 and S2; Saba, 2022) that the downward leader is highly branched (Figure 1b) and the branches alternate luminosity during their downward propagation. The upward leaders A and B respond to different downward propagating branches and, as the branches alternate in propagation and intensity, so do leaders A and B accordingly. However, during the last 100 μs, the alternation ceases, all downward leader branches intensify and consequently leaders A and B synchronize and pulse together. This period coincides with the rapid exponential growth of the DC base current (Figure 6, upper plot). It seems that the proximity of the downward leader branches is such that differences in leader branches propagation and intensities are not driving the upward leaders differently anymore.
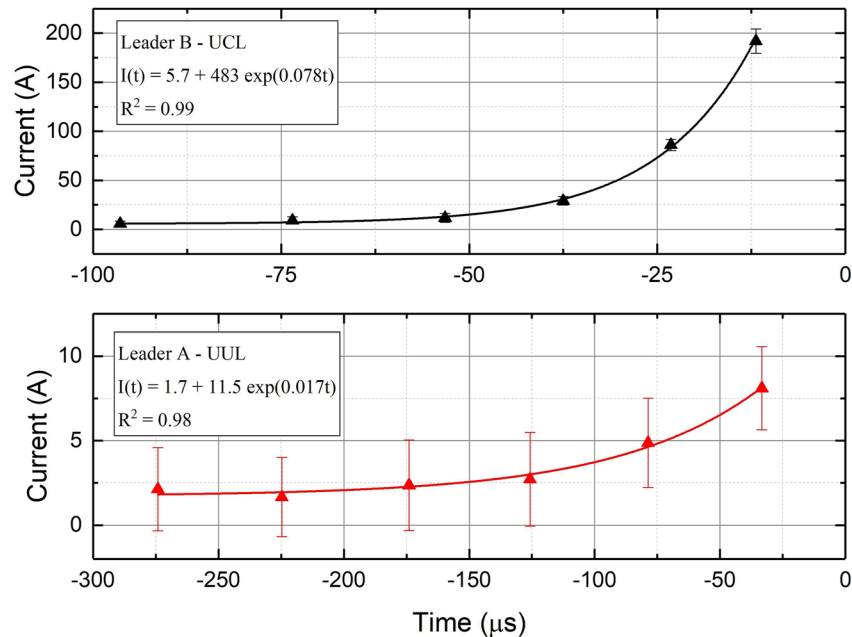
Figure 6. Exponential growth of the DC current measured for leader B (UCL, upper plot) and leader A (UUL, bottom).

4.4. Leader Charge Density and Charge Transfer

From the current and 2D leader length measurements it was possible to estimate how the transferred charge and the linear average charge density (ratio between the charge transferred and the upward leader length) of the leaders vary with time. In Figure 7 the continuous lines show the charge transferred by the upward leaders A and B and the triangles their average charge density during propagation. The charge and the charge density during the return stroke is not plotted for the UCL leader but its effects are seen in the charge and charge density plots of the UUL leader and will be addressed in the next section.

The charge densities of the leaders do not stay constant but increase rapidly with time during the propagation of the upward leaders (a similar result was obtained by Chen et al. (2013) for triggered lightning). This means that for both UUL and UCL the charge in the leader increases much faster than the length of the leader, which has an approximately constant speed as shown in Figure 5. Note also that the step like character of the charge variation is due to the current pulses during the leader propagation.
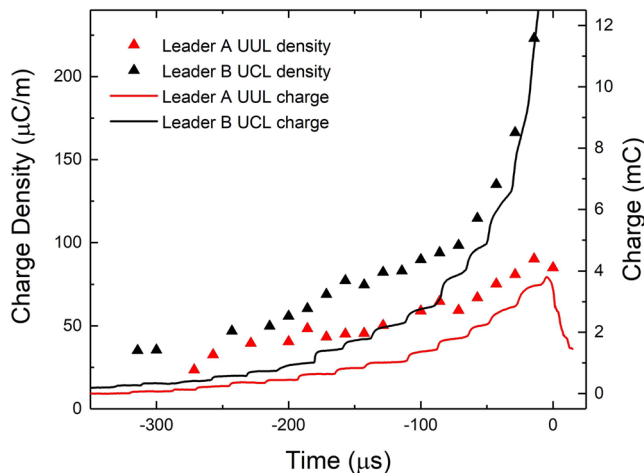

Figure 7. Average linear charge density and charge transferred by leaders A (UUL) and B (UCL).

4.5. Backflow Current

Approximately 500 μs after the attachment of the downward negative leader with leader B (UCL), when the intense luminosity of the return stroke subsides, no upward leaders are visible, meaning that they have all collapsed. The electric field that was driving the propagation of the UULs from several nearby structures collapses with the occurrence of the return stroke in B. Therefore, the charges contained in these leaders flow back to their origin in a very short time, creating an intense current in the opposite direction.

In fact, this can be observed in the current and charge transfer plots of leader A (UUL) in Figures 4 and 7 respectively. Note that once the attachment occurs (−14 μs < t < 0 s which corresponds to the integration time of image 24 in Figure 2), there is a current polarity reversal and charge transfer decrease. The reversed current of leader A (UUL) reaches a minimum of −701 A. This backflow current was modeled by Becerra and Cooray (2009)

Table 3
Characteristics of the Interval Between Pulses and Current Amplitude for Leaders A (UUL) and B (UCL)[a]

Parameter	Event	N	Min	Max	AM	DP	GM	MED
Interval between pulses (μs)	A (UUL)	13	16	33	24.2	5.2	23.6	24.0
	B (UCL)	17	14	29	22.8	4.4	22.4	23.0
	A and B	30	14	33	23.4	4.7	22.9	23.0
	Nag et al. (2021)	216	4.2	132.8	20.9	11.4	19.1	20.0
Current amplitude (A)	A (UUL)	18	18	149	76.1	37	66.3	71.0
	B (UCL)	18	21	413	145.7	124	99.3	102.5
	A and B	36	18	413	110.9	97	81.1	84.5
	Nag et al. (2021)	223	3.4	289.2	49.6	55.1	31.1	30.1

[a]*N is sample size, AM means arithmetic mean, DP is the standard deviation, GM is the geometric mean, and MED the median.*

and measured by Schoene et al. (2008), Visacro et al. (2010), and Nag et al. (2021) for structures with different heights (Table 2).

Table 2 also shows the height of the structure that starts the upward leader, the leader length, the total charge transferred, and linear charge density for leader A (UUL) and B (UCL). The length values of leaders A and B were estimated through the analysis of the frames acquired for the high-speed camera v12. Total charge was calculated through the integration of the current measurements up to the moment when the UUL starts to collapse (current reversion). In this table, we compare our values of positive leader linear charge density with estimated values by models or measured in some triggered lightning flashes and in laboratory discharge studies (no values were found in natural flashes studies).

4.6. Time Interval and Amplitude of Electric Field Changes and Current Pulses

The electric field measurements show abrupt negative changes that are synchronized with the occurrence of current pulses in upward leaders. The changes in the electric field produced by the positive upward leaders have the same orientation of the change produced by the negative return stroke. Positive charges are carried by the leaders over the electric field antenna in both cases. However, between the abrupt negative changes caused by the positive leaders, it is possible to see a slower positive change in the electric field due to the approach of the negative leader. As the positive charges displaced by the upward leaders are much closer to the electric field sensor than the negative charges of the downward leader, the overall change of the field prior to the return stroke is negative. Also, due to the larger distance from leader A to the field sensor, current pulses of leader A (red curve in Figure 4) produce smaller negative electric field changes than leader B pulses (black curve in Figure 4).
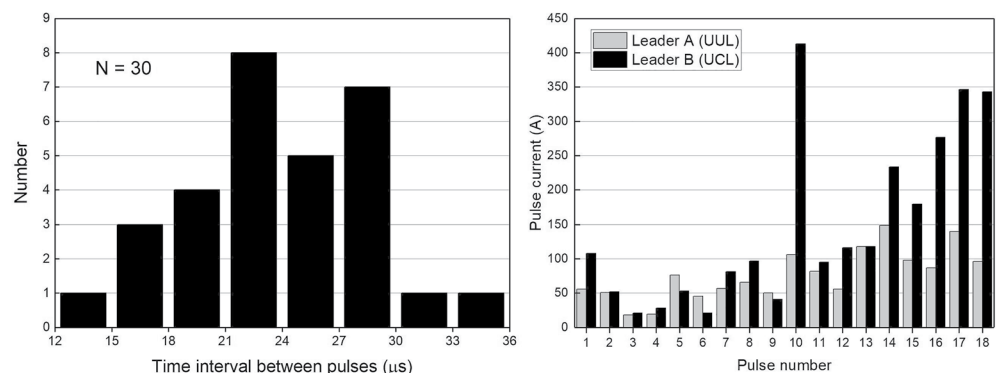

Figure 8. (a) Distribution of time intervals between pulses in leader A (UUL) and leader B (UCL); (b) peak current of pulses occurring during the initiation and progression of the leaders.

The average values of time interval between current pulses present in leader A and B are very similar, 24.2 and 22.8 μs respectively (see Table 3). If all intervals are considered, the average time interval between pulses is 23.4 μs with a standard deviation of 4.7 μs (see histogram of the distribution in Figure 8a). The average time interval between current pulses in leaders A and B (23.4 μs) is close to the interstep time interval found by optical or electric field sensors for negative cloud-to-ground stepped leaders (Hill et al., 2011; Krider et al., 1977; Lu et al., 2008). This strongly suggests that the current pulses present in upward leaders are induced by the electric field change produced by the steps in the propagation of the negative downward leader. Similar time intervals between the current pulses for UUL from a 91.5 m tall tower (Nag et al., 2021) are also shown in Table 3 for comparison. The time intervals between the current pulses from a 7 m tall structure observed by Schoene et al. (2008) (12–21 μs), and from a 60 m tall tower on top of a hill observed by Arcanjo et al. (2019) are also close to the average interstep time found in this work. However, as Arcanjo et al. (2019) filtered the pulses induced by all branches other than the main negative downward leader branch, the resulting time intervals obtained were higher (30–50 μs).

Table 3 also shows the current amplitude for leader pulses. In both leaders the amplitude of the pulses gets higher during the approach of the downward leader to the upward leaders (Figure 8b). The amplitude of the pulses present in leader B (UCL) are much more intense than those in leader A (UUL). The values obtained by Nag et al. (2021) for an instrumented 91.5 m tower are also presented for comparison. Note that the amplitudes observed by Nag et al. (2021) in seven UULs are lower than the ones obtained in the present study. This can be explained by the fact that in our study the downward leader that induced the upward leaders occurred overhead the instrumented lightning rods and produced a −73 kA peak current return stroke. In Nag et al. (2021), the downward leaders produced return strokes with peak currents ranging from −13 to −69.3 kA but at larger distances (hundreds of meters) from the instrumented tower.

5. Summary and Conclusion

In this study, for the first time, the current was measured simultaneously in two upward leaders during the attachment process of a downward negative leader. The connection took place with the lightning rod of a residential building and was simultaneously recorded with high-speed cameras, electric field sensor and current sensors giving the opportunity to compare the time interval between current pulses, the amplitude of the pulses and the behavior of the DC currents of an UCL and an UUL.

The approach of the negative downward leader induced 6 upward leaders prior to the return stroke. The brightest and longest ones were initiated from instrumented lighting rods and had their current intensities measured. One of them (from structure B, building P2) connected to the downward leader.

The downward leader and upward leaders A and B propagated at an approximately 2D constant speed, being the downward leader 2.0–5.5 times faster than the upward leaders and the UCL 17% faster than the UUL. The final jump speed (upward and downward leaders combined) is estimated to be at least 45 times faster than the average speed of the UCL prior to the jump. Although the peak current of the return stroke in this case was much higher than the previous ones analyzed by Saba et al. (2017) (Table S1 in Supporting Information S1), the speed ratios (V_d/V_{ucl} and V_d/V_{uul}) were similar. However, the charge of the downward leader, which is related to the intensity of the return stroke, may have influenced the speed of the upward leaders (all of them faster than previously reported cases). The faster speeds of the downward leader and the upward connecting leader reduced the time interval between the UCL leader inception and return stroke. The distance between the down-coming negative leader tip and the tip of the vertical rod at the inception of a stable upward positive leader (132 m) was not significantly different from previous cases (82, 120, and 62 m).

DC currents were measured during the propagation of both leaders (A and B). Both increased exponentially with a similar growth predicted by Becerra and Cooray (2009). The DC current of leader B (UCL) was much more intense than the DC current of leader A (UUL).

Pulses superimposed on the DC current of the upward leader were reported before. Although the amplitudes of the pulses are different in the case of taller structures (Visacro et al., 2010, tower height of 60 m over a 300 m tall mountain), the pattern of the pulses observed in this case is very similar to current measurements of UUL reported from tall towers (e.g., Figure 8 in Visacro et al., 2010), and from small structures (Figure 6 in Schoene et al., 2008, grounded vertical conductor of 7 m height over a flat terrain). Multiple current pulses occur from the lightning rods during the approach of the negative downward leader and the amplitude of the current pulses tend

to increase with time; the current peaks of the superimposed leader pulses range from 18 to 413 A; the pulses superimposed on UCL leaders are larger than the pulses superimposed on UUL leaders.

The average time interval between current pulses in upward leaders is close to the interstep time interval found by optical or electric field sensors for negative cloud-to-ground stepped leaders, which strongly suggests that the current pulses present in upward leaders are induced by the electric field change produced by the steps in the propagation of the negative downward leader.

The upward leaders A and B respond to different downward propagating branches and, as the branches alternate in propagation and intensity, so do leaders A and B accordingly. During the last 100 µs there is a rapid exponential growth of the DC base current, the alternation of the leaders ceases, all downward leader branches intensify and consequently leaders A and B synchronize and pulse together.

Although the leaders have an approximately constant speed, their linear charge density increases rapidly during their propagation. The total charge of the UCL is 5 times larger than the total charge of the UUL. The average linear densities for upward leaders (49 and 82 µC/m) were obtained for the first time for natural lightning. Previous measurements and estimations (from triggered lightning, laboratory measurements and theoretical studies) show values that range from half to 4 times higher.

The identification and characterization of the UCL and UUL reported here can help not only the understanding of the attachment process when several upward leaders are induced, but also the impact of these upward leaders in vulnerable equipment, in the ignition of flammable vapors and in injures caused to humans (Becerra & Cooray, 2009; Schoene et al., 2008).

Data Availability Statement

The high-speed videos analyzed in this work are available at (Saba, 2022): https://doi.org/10.5281/zenodo.7244891.

References

Arcanjo, M., Guimarães, M., & Visacro, S. (2019). On the interpeak interval of unipolar pulses of current preceeding the return stroke in negative CG lightning. *Electric Power Systems Research*, *173*, 13–17. https://doi.org/10.1016/j.epsr.2019.03.028

Becerra, M., & Cooray, V. (2009). On the interaction of lightning upward connecting positive leaders with humans. *IEEE Transactions on Electromagnetic Compatibility*, *51*(4), 1001–1008. https://doi.org/10.1109/TEMC.2009.2033265

Chen, M., Zheng, D., Du, Y., & Zhang, Y. (2013). Evolution of line charge density of steadily-developing upward positive leaders in triggered lightning. *Journal of Geophysical Research: Atmospheres*, *118*(10), 4670–4678. https://doi.org/10.1002/jgrd.50446

Cooper, M. A., & Holle, R. L. (2019). *Reducing lightning injuries worldwide*. Springer. https://doi.org/10.1007/978-3-319-77563-0

Hill, J. D., Uman, M. A., & Jordan, D. M. (2011). High-speed video observations of a lightning stepped leader. *Journal of Geophysical Research*, *116*(16), 1–8. https://doi.org/10.1029/2011JD015818

Krider, E. P., Weidman, C. D., & Noggle, R. C. (1977). The electric field produced by lightning stepped leaders. *Journal of Geophysical Research*, *82*(6), 951–960. https://doi.org/10.1029/jc082i006p00951

Les Renardières, G. (1977). Positive discharges in long air gaps at Les Renardières—1975. *Electra*, *53*.

Lu, W., Chen, L., Ma, Y., Rakov, V. A., Gao, Y., Zhang, Y., et al. (2013). Lightning attachment process involving connection of the downward negative leader to the lateral surface of the upward connecting leader. *Geophysical Research Letters*, *40*(20), 5531–5535. https://doi.org/10.1002/2013GL058060

Lu, W., Gao, Y., Chen, L., Qi, Q., Ma, Y., Zhang, Y., et al. (2015). Three-dimensional propagation characteristics of the leaders in the attachment process of a downward negative lightning flash. *Journal of Atmospheric and Solar-Terrestrial Physics*, *136*, 23–30. https://doi.org/10.1016/j.jastp.2015.07.011

Lu, W., Wang, D., Takagi, N., Rakov, V., Uman, M., & Miki, M. (2008). Characteristics of the optical pulses associated with a downward branched stepped leader. *Journal of Geophysical Research*, *113*(21), 1–9. https://doi.org/10.1029/2008JD010231

Naccarato, K. P., De Paiva, A. R., Saba, M. M. F., Schumann, C., Silva, J. C. O., & Ferro, M. A. S. (2017). Preliminary comparison of direct electric current measurements in lightning rods and peak current estimates from lightning location systems. In *2017 international symposium on lightning protection, XIV SIPDA* (pp. 319–323). https://doi.org/10.1109/SIPDA.2017.8116944

Naccarato, K. P., Saraiva, A. C. V., Saba, M. M. F., & Schumann, C. (2012). First performance analysis of BrasilDAT total lightning network in southeastern Brazil. In *International conference on grounding and earthing & 5th international conference on lightning physics and effects* (p. 6).

Nag, A., Cummins, K. L., Plaisir, M. N., Wilson, J. G., Crawford, D. E., Brown, R. G., et al. (2021). Inferences on upward leader characteristics from measured currents. *Atmospheric Research*, *251*, 105420. https://doi.org/10.1016/j.atmosres.2020.105420

Rizk, F. A. M. (1990). Modeling of transmission line exposure to direct lightning strokes. *IEEE Transactions on Power Delivery*, *5*(4), 1983–1997. https://doi.org/10.1109/61.103694

Rizk, F. A. M. (1994). Modeling of lightning incidence to tall structures Part I: Theory. *IEEE Transactions on Power Delivery*, *9*(1), 162–171. https://doi.org/10.1109/61.277673

Saba, M. M. F. (2022). Supplementary data for "Upward leaders from instrumented lightning rods competing to connect a downward leader during a lightning attachment process" [Dataset]. Zenodo. https://doi.org/10.5281/ZENODO.7244891

Saba, M. M. F., Paiva, A. R., Schumann, C., Ferro, M. A. S., Naccarato, K. P., Silva, J. C. O., et al. (2017). Lightning attachment process to common buildings. *Geophysical Research Letters*, *44*(9), 4368–4375. https://doi.org/10.1002/2017GL072796

Saba, M. M. F., Schumann, C., Warner, T. A., Helsdon, J. H., & Orville, R. E. (2015). High-speed video and electric field observation of a negative upward leader connecting a downward positive leader in a positive cloud-to-ground flash. *Electric Power Systems Research*, *118*, 89–92. https://doi.org/10.1016/j.epsr.2014.06.002

Saba, M. M. F., Silva, D. R. R., Pantuso, J. G., & Silva, C. L. (2022). Close view of the lightning attachment process unveils the streamer zone fine structure. *Journal of Geophysical Research*, *49*(24), e2022GL101482. https://doi.org/10.1029/2022GL101482

Schoene, J., Uman, M. A., Rakov, V. A., Jerauld, J., Hanley, B. D., Rambo, K. J., et al. (2008). Experimental study of lightning-induced currents in a buried loop conductor and a grounded vertical conductor. *IEEE Transactions on Electromagnetic Compatibility*, *50*(1), 110–117. https://doi.org/10.1109/TEMC.2007.911927

Tran, M. D., & Rakov, V. A. (2017). A study of the ground-attachment process in natural lightning with emphasis on its breakthrough phase. *Scientific Reports*, *7*(1), 1–13. https://doi.org/10.1038/s41598-017-14842-7

Visacro, S., Guimaraes, M., & Murta Vale, M. H. (2017a). Features of upward positive leaders initiated from towers in natural cloud-to-ground lightning based on simultaneous high-speed videos, measured currents, and electric fields. *Journal of Geophysical Research: Atmospheres*, *122*(23), 12786–12800. https://doi.org/10.1002/2017JD027016

Visacro, S., Guimaraes, M., & Murta Vale, M. H. (2017b). Striking distance determined from high-speed videos and measured currents in negative cloud-to-ground lightning. *Journal of Geophysical Research: Atmospheres*, *122*(24), 13356–13369. https://doi.org/10.1002/2017JD027354

Visacro, S., Murta Vale, M. H., Correa, G., & Teixeira, A. (2010). Early phase of lightning currents measured in a short tower associated with direct and nearby lightning strikes. *Journal of Geophysical Research*, *115*(D16104), 1–11. https://doi.org/10.1029/2010JD014097